Time and Frequency Domain Measurements of Ferromagnetic Resonance in Small Spin-Valve

Stephen E. Russek and Shehzaad Kaka

***Abstract*—Time and frequency domain magnetoresistance measurements of ferromagnetic resonance (FMR) in small spin-valve devices are presented along with comparisons to single-domain simulations. The measurements and simulations give consistent results for rotational motion with angular deviations of less than 30° from the easy axis. While the time and frequency domain measurements produce similar results for ideal devices in the linear regime, each technique provides different information as the devices become nonlinear and less ideal. Both time and frequency domain magnetoresistance measurements allow the study of FMR in considerably smaller magnetic structures than can be done with conventional techniques.**

***Index Terms*—FMR, GMR, magnetic device dynamics, MRAM, spin-valve.**

I. INTRODUCTION

GIANT magnetoresistance (GMR) and magnetic tunnel junction devices being developed for data storage applications such as magnetic recording read sensors and magnetic random access memory will soon be required to operate at gigahertz frequencies [1], [2]. This operation frequency is near the ferromagnetic resonance (FMR) of these devices. Detailed measurements and understanding of FMR in small devices will be required if this effect is to be used constructively to enhance the output signal of a magnetic sensor or to switch a magnetic device more efficiently.

We have measured the ferromagnetic resonance in a small spin-valve device using both pulsed time-domain and swept-frequency techniques. Both techniques measure the device response in the gigahertz frequency range and are, in principle, equivalent when the device is operating in the linear regime and is well behaved (no Barkhausen noise). In practice, the two are not equivalent since they respond to nonlinearities and nonideal behavior differently, create different heating and parasitic effects, and have different measurement problems that determine their signal-to-noise performance.

II. EXPERIMENT

Spin-valve devices were fabricated by optical lithography and incorporated into a microwave measurement circuit that uses integrated microstrip field and sense lines to deliver magnetic field excitations and measure the high-frequency response of the device [3]. The device dimensions are $0.8\ \mu\mathrm{m} \times 4.8\ \mu\mathrm{m}$

Manuscript received February 15, 2000. This work was supported by the DARPA Spintronics program and NIST ATP.

The authors are with the National Institute of Standards and Technology, Boulder, CO 80303 USA (e-mail: {russek; shehzaad}@boulder.nist.gov).

Publisher Item Identifier S 0018-9464(00)08961-5.

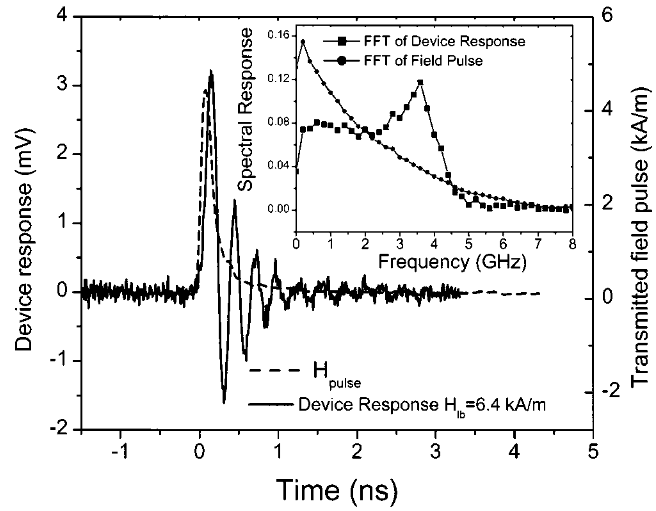

Fig. 1. Transmitted magnetic field pulse and device response for a $4.8\ \mu\mathrm{m} \times 0.8\ \mu\mathrm{m}$ spin-valve device with 6.4 kA/m longitudinal bias field. The inset shows the FFT of both signals. The FFT of the device response clearly shows the ferromagnetic resonance at 3.6 GHz.

and have a layer structure of Ta 5.0 nm - $Ni_{0.8}Fe_{0.2}$ 5.0 nm - Co 1.0 nm-Cu 3.0 nm-Co 2.0 nm-Ru 0.6 nm-Co 1.5 nm - FeMn 10 nn - Ta 5.0 nm. The pin direction was set 90° to the long (easy) axis of the device and was measured to be within 3° of the nominal set direction. The pinning field is >100 kA/m and the pinned layer undergoes little dynamical motion for the field excitations used in this study. The measured voltage (relative to the quiescent bias voltage) is proportional to the average transverse magnetization of the free layer, M_y, between the contact leads and may be determined by $M_y/M_s = V_{resp}/V_{sat}$, where M_s is the saturated magnetization of the free layer, V_{resp} is the measured voltage, and V_{sat} is the measured saturation voltage at high applied fields.

The time-domain measurements were made by sending a voltage pulse down the field line, which produces a magnetic field pulse along the hard axis, perpendicular to the long axis of the device. The transmitted field pulse was monitored using a 20 GHz bandwidth sampling oscilloscope. The incident pulse had a full width at half maximum (FWHM) of 100 ps and the transmitted pulse had a FWHF of $t_{pw} = 160$ ps (see Fig. 1). The approximate field-pulse amplitude is calculated from the measured voltage using $H_{pulse} = V_{tran}/2Zw$, where V_{tran} is the measured voltage, Z is the microstrip impedance, and w is the width of the microstrip line. The maximum field-pulse amplitude for these time domain studies was 4.5 kA/m. A 1 mA bias current was applied to the device and the high frequency voltage response was taken off through a bias tee and sent

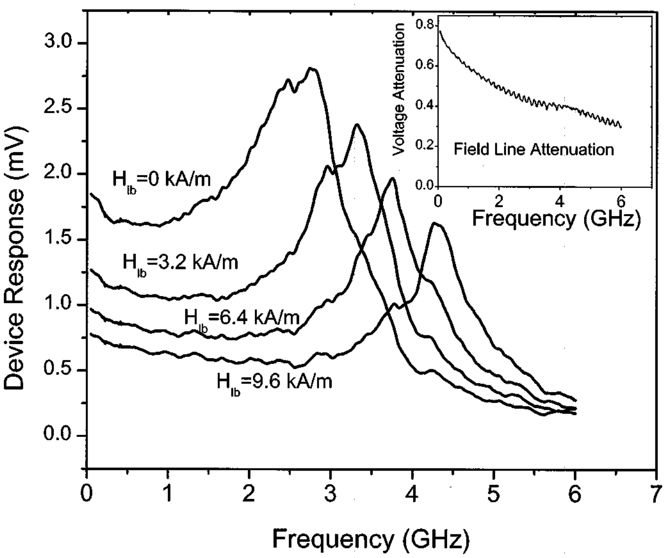

Fig. 2. Spin-valve response measured in the frequency domain for several values of longitudinal bias field. The FMR shifts to higher frequencies and the response amplitude decreases as the longitudinal bias field is increased. The inset shows the frequency-dependent attenuation for the field line.

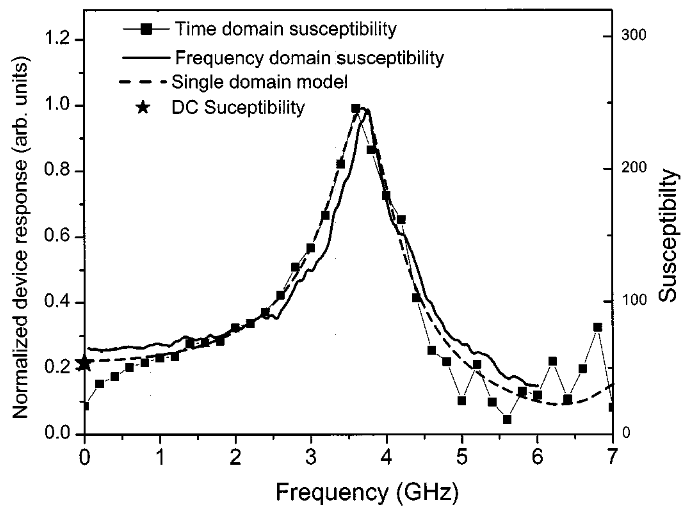

Fig. 3. Normalized time and frequency-domain device response and magnetic suspectibility calculated from a single-domain Landua–Liftshiz simulation. The simulation assumes a device size of $0.95\ \mu\mathrm{m} \times 4.8\ \mu$m, $\alpha = 0.03$, and bulk magnetization values. Also shown is the measured DC suspectibility.

into a broadband microwave amplifier and then to a 20 GHz sampling oscilloscope.

The frequency-domain measurements were made on the identical device with the same setup, except that the field line was driven by the output of a 20 GHz network analyzer, and the device signal, after the sense amplifier, was sent into the second port of the network analyzer. The microwave power was fixed at 10 mW, which corresponds to a rms field of 1.8 kA/m.

For both measurements a background signal arises from capacitive coupling from the field line to the device and sense line. The background signal is measured with no current through the device and is subtracted from the signal with current flowing. For the real-time measurements, the background correction is a scalar subtraction. For the frequency-domain measurements, the correction is a subtraction of the complex Fourier amplitudes.

III. Results

Fig. 1 shows the transmitted applied-field pulse and time-domain response of the spin-valve device with 6.4 kA/m longitudinal bias field (along the easy axis of the device). The response is consistent with earlier measurements on similar devices [4]. The measured peak voltage yields a maximum value of the transverse magnetization of $M_y M_s = 0.45$, which corresponds to a rotation angle of 27°. The inset shows the fast Fourier transform (FFT) of the field pulse and device response. The FFT of the field pulse has a FWHM of 1.4 GHz. The FFT of the device response shows a resonance at 3.60 GHz. The resonant response is excited because the driving pulse contains a significant component at the resonant frequency.

Fig. 2 shows the frequency-domain response for several values of the longitudinal bias field, H_{lb}. As the longitudinal bias is increased, the resonance amplitude shifts to higher frequencies and the response amplitude decreases. These results are in qualitative agreement with simple single-domain models which predict, for small rotation angles,

$$f_r = \gamma\sqrt{M_s(K_k + H_{lb})}, \quad V_{resp} \propto H_{pulse}/(H_k + H_{lb}),$$

where H_k is the anisotropy field due to shape anisotropy. The inset in Fig. 2 shows the measured voltage attenuation for the field line, which indicates that a considerable amount of the fall-off in the device response at high frequencies is due to attenuation of the drive field.

To compare the time-domain and frequency-domain data, we compute the normalized device response, which is proportional to the magnetic susceptibility χ_m, by dividing the FFT of the time-domain device response by the FFT of the transmitted field pulse. For the frequency-domain data, we divide the device response by the frequency-dependent attenuation of the field line. Both the time and frequency domain data are further normalized by dividing by the maximum value at resonance. This normalized device response is plotted in Fig. 3.

Also shown in Fig. 3 is the susceptibility calculated from a single-domain Landau–Lifshitz simulation of a spin-valve driven by a 160 ps 4.8 kA/m magnetic field pulse. The simulation assumes the device is a rectangular prism and calculates the demagnetizing factors using the analytic expression given in [5]. The free-layer magnetization is assumed to be 837 kA/m, which is the thickness-weighted average of the $Ni_{0.8}Fe_{0.2}$ and Co layers, assuming bulk magnetization values and a 0.5 nm dead layer at the $Ni_{0.8}Fe_{0.2}$–Ta interface. The damping parameter a is adjusted to fit the data and is 0.03 for the simulation shown in Fig. 3. If nominal device dimensions of $0.8\ \mu\mathrm{m} \times 4.8\ \mu$m are assumed, the simulations give $H_k = 11.4$ kA/m, $\chi_{mDC} = 49$, and $f_r = 3.9$ GHz, where χ_{mDC} is the DC susceptibility. To get agreement with the measured data, we need to artificially soften the single-domain response by increasing the device width to 0.95 μm. The simulated H_k, χ_{mDC} and f_r then agree reasonably well with

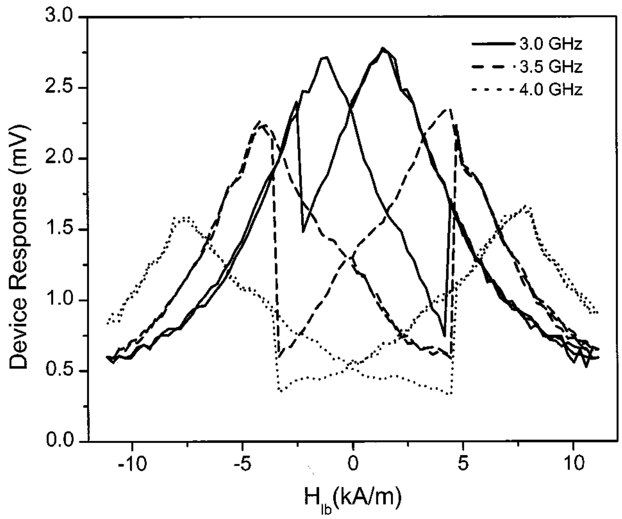

Fig. 4. Device response versus longitudinal magnetic field for several fixed frequencies. The free layer switches at ~3–4 kA/m and the switching field is dependent on the response amplitude.

the measured values of $H_k = 8.4$ kA/m, $\chi_{mDC} = 54$, and $f_r = 3.6$ GHz.

The ferromagnetic resonance can also be measured by applying a fixed microwave frequency and measuring the device response as the longitudinal bias field is varied. This data is shown in Fig. 4 for excitation frequencies of 3.0 GHz, 3.5 GHz, and 4.0 GHz. At approximately 3 kA/m to 4 kA/m, the device free layer switches to its other stable state. There is some dependence of the switching field on the amplitude of the device response, with the switching field decreasing as the excitation frequency decreases and the response increases. The width of the 3 GHz FMR peak is 7.6 kA/m, which is consistent with the single-domain simulations, which predict a line width of 9.4 kA/m using an $\alpha = 0.03$.

IV. Discussion

The time and frequency domain data in Fig. 3 show reasonable agreement for the small excitation fields used. Simulations show that, for the range of field excitations used here, $0.2 < H_{pulse}/H_k < 0.54$, the expected variation in the suspectibility is less than 1% at 1 GHz and less than 6% at resonance. As the excitation field is increased linear analysis will no longer apply and the time and frequency domain measurements will no longer agree. For large field amplitudes, response at higher frequencies, particularly at the resonant frequency, can be simulated even when the driving field has no Fourier components in these higher frequency ranges. At very high transverse-field amplitudes, the device can be driven into a metastable state where the center of teh device has reversed and the device edges are still pinned in the original direction [6]. This type of nonlinear dynamics is more clearly measured in the time domain and would be difficult to characterize in the frequency domain.

An exact measurement of the high-frequency suspectibility of small devices is difficult because the microstrip lines are lossy due to their small dimensions (2 μm and 4 μm widths respectively). There are large frequency-dependent attenuations as seen in Fig. 2 inset. Here we normalized both the time and frequency domain data to the transmitted microwave signal coming out of the field line and did not account for frequency-dependent attenuation of the device signal. A quantitative measurement of the susceptibility would require an accurate determination of the frequency-dependent field amplitude at the device location and the frequency-dependent losses in the sense line.

In summary, measurements of the ferromagnetic resonance in small spin-value devices have been made in the time and frequency domains by using the magnetoresistance to monitor the magnetization of the device. This technique is more sensitive than other micro-FMR techniques [7] and can be scaled to measure FMR in device structures down to 50 nm diameter and 2 nm film thickness. Further, it allows continuous characterization from the linear to the highly nonlinear regime, where switching and metastable state formation occur.

References

[1] K. B. Klaassen, R. G. Hirko, and J. T. Conteras, "High speed magnetic recording," *IEEE Trans. Magn.*, vol. 34, pp. 1822–1827, July 1998.

[2] R. H. Koch, J. G. Deak, D. W. Abraham, P. L. Trouilloud, R. A. Altman, Y. Lu, W. J. Gallagher, R. E. Scheuerlein, K. P. Roche, and S. S. P. Parkin, "Magnetization reversal in micron-sized magnetic thin films," *Phys. Rev. Lett.*, vol. 81, pp. 4512–4515, Nov. 1998.

[3] S. E. Russek, J. O. Oti, S. Kaka, and E. Y. Chen, "High-speed characterization of sub-micrometer giant magnetoresistive devices," *J. Appl. Phys.*, vol. 85, pp. 4773–4775, April 1999.

[4] S. E. Russek, S. Kaka, and M. Donahue, "High-speed dynamics, damping, and energy relaxation times in submicrometer spin-valve devices," *J. Appl. Phys.*, vol. 87, pp. 7070–7072, March 2000.

[5] A. Aharoni, "Demagnetizing factors for rectangular ferromagnetic prism," *J. of Appl. Phys.*, vol. 83, pp. 3432–3434, March 1998.

[6] P. Kabos, T. Silva, and S. E. Russek, "Metastable states in large angle magnetic rotations,", these proceedings.

[7] S. Zhang, S. A. Oliver, N. E. Israeloff, and C. Vittoria, "High-sensitivity ferromagnetic resonance measurements on micrometer sized samples," *Appl. Phys. Lett.*, vol. 70, pp. 2756–2758, May 1997.